

The proper motion distance to the remarkable bipolar planetary nebula KjPn 8

J. Meaburn

Department of Physics and Astronomy, University of Manchester, Oxford Road, Manchester M13 9PL

Accepted 1997 September 9. Received 1997 August 29; in original form 1997 July 14

ABSTRACT

The expansion proper motions of the high-speed groups of knots A1 and A2 at the tips of the inner bipolar lobes of the extraordinary bipolar nebula KjPn 8 have been measured as 34 ± 3 mas yr⁻¹ by comparing their images on a Palomar Observatory Sky Survey 1954 plate with one taken in 1991. This value has been used within a bowshock model for the generation of the emission line knots to derive a distance to KjPn 8 of $D = 1600 \pm 230$ pc. A kinematical age of $T = 3400 \pm 300$ yr for the two groups of knots is given directly by this measurement of proper motion and the 115-arcsec projected angular distance of the knots from the nebular core.

Key words: planetary nebulae: individual: KjPn 8.

1 INTRODUCTION

The bipolar planetary nebula (PN) KjPn 8, with its 14×4 arcmin² filamentary lobes, yet only 4-arcsec diameter bright core, is the most extraordinary one of this type yet discovered at optical wavelengths (López, Vasquez & Rodríguez 1995). Only the somewhat smaller (11×4 arcmin²) but similar He2 111 offers any competition for this accolade (Webster 1978; Meaburn & Walsh 1989). The point symmetric groups of the ionized knots marked A1 and A2, B1 and B2 and possibly C1 and C2 in the sketch of KjPn 8 in Fig. 1 suggest (López et al. 1995) the action of a rotating (or wandering) episodic jet from the central source similar to that proposed for the PN Fleming 1 (López, Roth & Tapia 1993a; López, Meaburn & Palmer 1993b). Certainly the discovery of bipolar outflow speeds of ≈ 320 km s⁻¹ for the knots A1 and A2 shown in the [N II] $\lambda 6548$ -Å CCD images of López et al. (1995) [see the enlargements from these in Figs 2(a) and (b), opposite p. L12, respectively] helps to substantiate this suggestion (López et al. 1997a). Moreover, the H α and [N II] $\lambda 6584$ -Å line profiles from A1 and A2 have the characteristics expected for their generation by radiative bow shocks as ejected ‘bullets’ plough through ambient gas.

Further interest in KjPn 8 has been stimulated by the discovery by Huggins et al. (1997) of a 20-arcsec molecular disc centred on the compact nebular core but with an axis that is aligned with the most recent bipolar outflows (A1 and A2 in Fig. 1).

The vital distances of PNe beyond the range of parallax measurements are notoriously difficult to derive. A direct

method is to measure the proper motions (PMs) of their expanding envelopes. The high-resolution Very Large Array radio measurements of Hajian & Terzian (1996) exploit this technique for bright PNe with well-defined expansions of a few tens of km s⁻¹ of their ionized cores. The detection of the knots A1 and A2 in Fig. 1 by the 1954 and 1991 Palomar Observatory Sky Surveys (POSS) when combined with the previous (López et al. 1997a) velocity measurements (hundreds of km s⁻¹) has provided an opportunity to apply a variation of the PM distance technique to this intriguing bipolar PN, KjPn 8.

2 PROPER MOTION MEASUREMENTS OF A1 AND A2

The images of the groups of emission line knots A1 and A2 are present on the film copies of the POSS E plate taken on 1954 August 7/8 and the corresponding POSS R plate taken on 1991 August 8, i.e. 37.00 yr apart. The bandwidths for these observations were ≥ 50 times the 10-Å bandwidth for the [N II] $\lambda 6548$ -Å CCD images in Figs 2(a) and (b), consequently many more confusing stellar images are present. However, parts of A1 and A2, emitting the dominant nebular H α and [N II] $\lambda 6584$ -Å lines, have been detected nearly equally on these two POSS plates. Any angular displacements of nebular features between the E and R POSS plates cannot be a result of unequal transmission of emission lines.

For the present PM measurements, small areas covering knots A1 and A2 of both the 1954 and 1991 POSS film copies were copied on to fine grain film with an enlargement

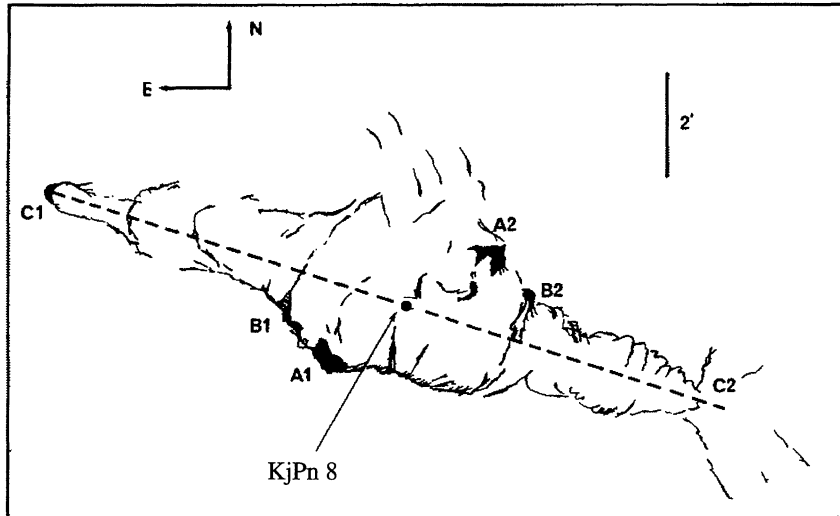


Figure 1. A sketch of the bipolar lobes surrounding the PN, KJpN 8. The point symmetric groups of knots A1 and A2, B1 and B2 and C1 and C2 (from López et al. 1995) are indicated as is the axis (dashed line) of the largest bipolar structure.

of 3.1 times. These enlarged films were then digitized with the PDS scanning microdensitometer at the Royal Greenwich Observatory. Data were read out every $15\ \mu\text{m}$ ($\equiv 0.32 \pm 0.01$ arcsec) along an individual scan which was separated from the next again by $15\ \mu\text{m}$. Each of the four resultant data arrays, i.e. 1954A1, 1991A1, 1954A2 and 1991A2, contained 1000×1000 pixels.

After this process there were significant variations in scale, centering and orientation between the corresponding 1954 and 1991 arrays. These differences were reduced to negligible proportions by use of Starlink CCDALIGN software on the Manchester Starlink data processing node. For the alignment of arrays 1954A1 and 1991A1, the images of 14 faint reference stars surrounding the knots A1 were used. These stellar images were not saturated and being of distant stars had negligible proper motions (PMs) themselves. Corresponding images of individual faint stars in both arrays after this alignment process in the vicinity of the knots A1 had centroids aligned to ≤ 0.1 arcsec. The overall error introduced by array misalignments to the subsequent nebular PM measurements is completely negligible. A similar process using 31 faint reference stellar images was used to align array 1954A2 with 1991A2.

The corresponding pairs of aligned data arrays were first examined using the ‘blink’ software in the Starlink GALA package. The groups of knots A1 and A2 could be seen to have moved globally a significant angular distance away (≈ 1 arcsec) from the core of KJpN 8 (see Fig. 1) between 1954 and 1991, whereas the ‘blinked’ stellar images in the same fields remained stationary.

Areas of the data arrays both free of stellar images and with nebular features of small angular width in the direction of motion were needed to permit a sufficiently accurate measurement of the PMs of A1 and A2. These criteria were satisfied best for the filament indicated by an arrow in Fig. 2(a), the contours of which, from 1954A1 and 1991A1, are shown in Figs 3(a) and (b) respectively. The dashed line in both Figs 3(a) and (b) is in the same place and perpendicular to the line to the core of KJpN 8. A displacement of the

filament between 1954 and 1991 outwards along this direction of 1.25 ± 0.1 arcsec has occurred. The PM from the nebular centre is then 34 ± 3 mas yr $^{-1}$. This measurement was made by shifting the contours of the whole feature in the 1954 array until they became centred by eye on those in the 1991 array. The quoted error is conservatively large. A similar outward displacement can be seen in Figs 4(a) and (b) for the somewhat broader and more complex feature in the A2 group of knots which is indicated by an arrow in Fig. 2(b). An angular displacement of the same magnitude as that for the A1 knot, but in the opposite direction, can be seen, but any measurement errors would be far larger, for the image of the knot has rotated somewhat between these dates. Only the more accurate measurement of the PM for the A1 knot will be used here.

3 THE DISTANCE TO KJpN 8

An estimation of the PM distance, D , to KJpN 8 depends on a sound estimation of the tangential expansion velocity, V_t , of the A1 knots in Figs 3(a) and (b), for

$$D(\text{pc}) = 0.2168 V_t(\text{km s}^{-1}) / \text{PM}(\text{arcsec yr}^{-1}). \quad (1)$$

The previously reported (López et al. 1997a) H α and [N II] $\lambda 6584\text{-\AA}$ line profiles from the groups of knots A1 and A2 revealed bright components with large radial velocity differences with respect to the systemic, heliocentric radial velocity, $V_{\text{SYS}} = -44$ km s $^{-1}$, yet continuous to this value. The generation of the line emission by overlapping radiative bow shocks is strongly suggested. Multiple bullets in each group of knots appear to be ploughing into the surface of the largest (14-arcmin long) bipolar feature which is expanding away from its axis (shown as a dashed line in Fig. 1) at 40 km s $^{-1}$. Hartigan, Raymond & Hartmann (1987) have shown that for such radiative bow shocks, the shock velocities in the ambient gas are given by the full width zero intensities (FWZIs) of the line profiles now measured as 267 km s $^{-1}$ for knots A1 and 280 km s $^{-1}$ for knots A2. In this case, the outflow velocities of the A1 knots must be ≈ 307

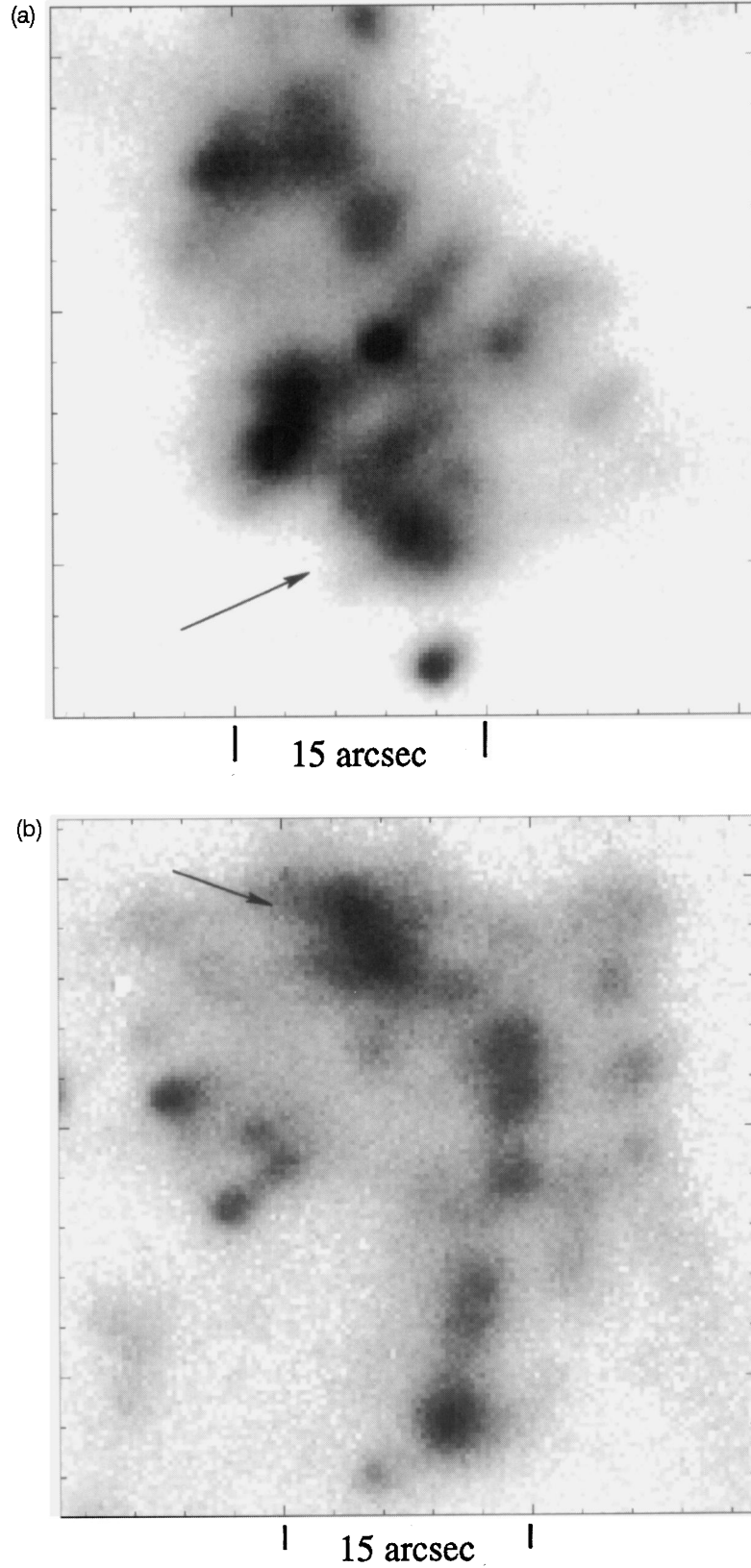


Figure 2. (a) An [N II] $\lambda 6548\text{-}\text{\AA}$ CCD image of the A1 group of knots identified in Fig. 1. This was obtained by J. A. López in 1994 September. The filament indicated by an arrow is that shown from the POSS images in Figs 3(a) and (b). (b) An [N II] $\lambda 6548\text{-}\text{\AA}$ CCD image of the A2 group of knots identified in Fig. 1. The knot shown by the arrow is that shown from the POSS images in Figs 4(a) and (b).

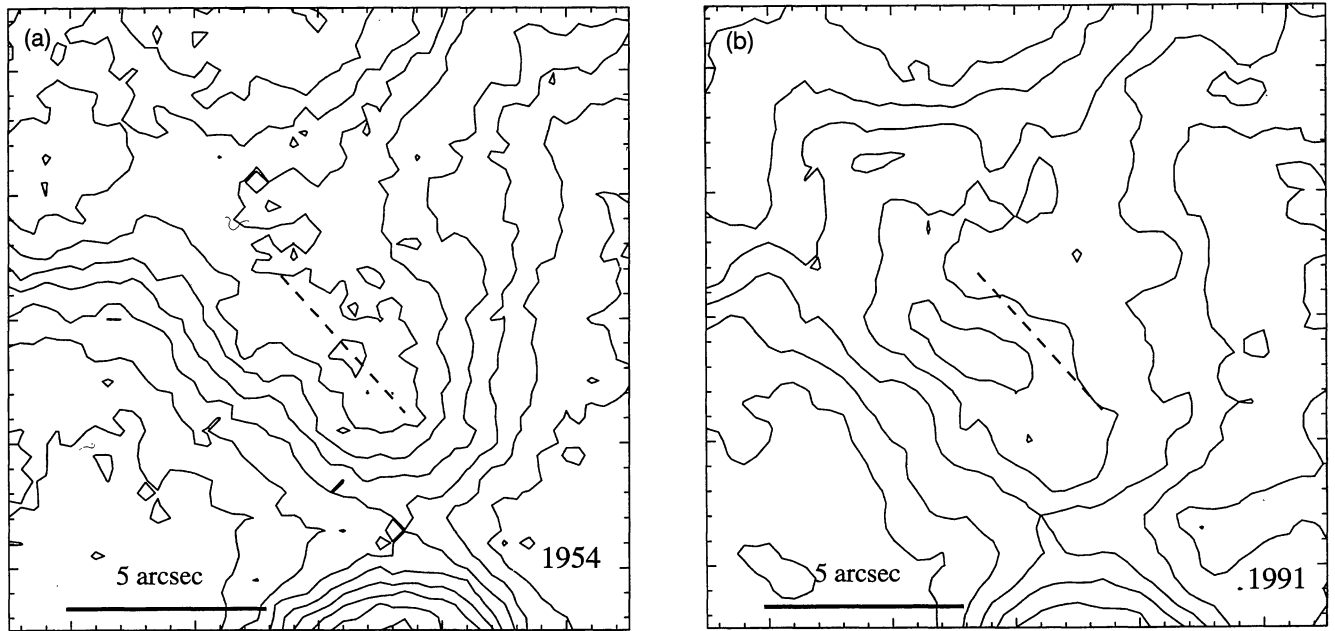


Figure 3. (a) A contour map, with linear intervals of photographic density, of the microdensitometer scan of the filament indicated in Fig. 2(a) in the A1 group of knots. This is from the 1954 POSS film copy. For reference, a dashed line indicates the approximate centre of the brightness ridge and is orientated perpendicularly to the direction of the nebular core. (b) A contour map with linear intervals of the microdensitometer scan of the same filament indicated in Fig. 2(a) from the 1991 POSS film copy. The dashed line is in the same position as for Fig 3(a). The coordinates of the 1954 and 1991 arrays have been made similar to a high degree of accuracy for this comparison. A significant shift of the filaments can be appreciated.

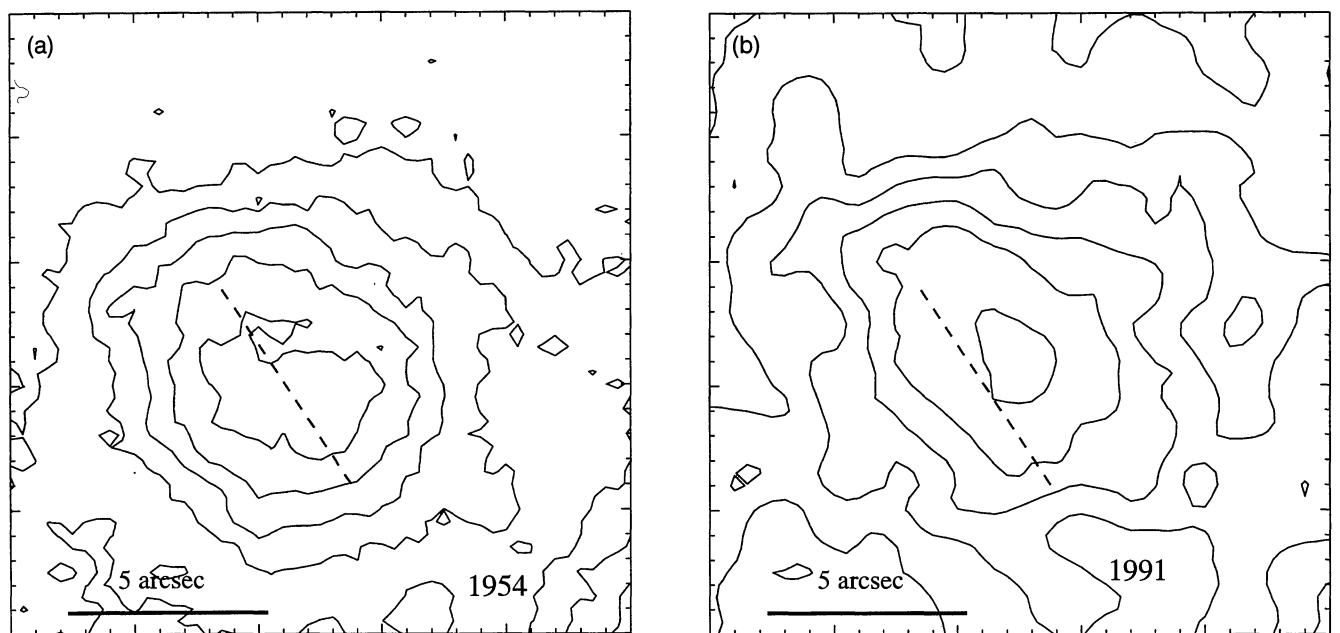


Figure 4. As for Fig. 3 but for the knot shown by the arrow in Fig. 2(b) in the A2 group of knots.

km s^{-1} and of the A2 knots $\approx 320 \text{ km s}^{-1}$, which takes into account the expansion velocity of the surface into which they are moving. An estimation of V_i for substitution into equation (1) can now be made from the radial velocity difference (blue-shifted) of 200 km s^{-1} of the peaks of the A1 line profiles with respect to V_{SYS} and of 160 to 200 km s^{-1}

(red-shifted) for the A2 line profiles. The strong symmetry of the images of A1 and A2 (see Fig. 1) and of the line profiles suggests that the most reasonable approach is to assume that A1 and A2 are travelling along a common axis tilted at θ with respect to the plane of the sky and with the same outflow velocity. Consequently, using the mean values

of the velocity measurements, $\sin(\theta) = 187/314$ to give $\theta = 37^\circ$ and $V_i = 251 \pm 20 \text{ km s}^{-1}$. By substitution of the measured values of V_i and PM into equation (1), the distance of KjPn 8 is $D = 1600 \pm 230 \text{ pc}$ when all the uncertainties are considered.

4 DISCUSSION

First, a straightforward estimation of the kinematical age, T , of the symmetric groups of knots A1 and A2 can now be made if their outflow speeds have been constant since their ejection from the core of KjPn 8. Their angular distances from this core can be seen in Fig. 1 to be 115 arcsec; therefore, with an expansion $\text{PM} = 34 \pm 3 \text{ mas yr}^{-1}$, $T = 3400 \pm 300 \text{ yr}$.

An immediate implication of $D = 1600 \pm 230 \text{ pc}$ is that the $14 \times 4 \text{ arcmin}^2$ lobes (culminating in C1 and C2 in Fig. 1) have linear dimensions of $6.5 \times 1.9 \text{ pc}^2$ as the kinematical evidence (López et al. 1997a) suggests that their axis (dashed line in Fig. 1) is nearly in the plane of the sky. These are then extraordinarily large features to be associated with a PN whose bright core at this distance (marked as KjPn 8 in Fig. 1) has a diameter typical for a PN of 0.03 pc. Incidentally, the estimation of the mass of the CO emitting disc now becomes $\approx 0.02 M_\odot$ from the measurements of Huggins et al. (1997), which is about 1/5th of the ionized mass usually estimated to be in the bright shells of PNe.

As with all distance measurements to PNe that do not depend on measurements of the parallax of their central stars, the reality of the present PM distance should be questioned. For instance, $D = 1600 \text{ pc}$ appears inconsistently large compared with $D \leq 1.0 \text{ kpc}$ derived from the measurements of $E(B - V) = 0.51$ from the thermal radio/H β intensity ratio of the nebular core (López et al. 1995). However, the scattering and absorbing clouds along the galactic plane are very patchy, consequently large inconsistencies occur with the application of this extinction method.

The weakness of the present PM distance measurement is that the estimation of V_i is dependent on the application of a bowshock model for the groups of knots A1 and A2. However, some confidence that this model does apply comes from the detailed modelling of the morphology and kinematics of the point symmetric knots on either side of the PN, HB4 (López et al. 1997b). In this far less complex

situation, very convincing fits to the kinematical predictions of bowshock models are achieved. Furthermore, the position of the images of the groups of knots A1 and A2 well away from the nebular core (see Fig. 1), when combined with the direct measurements of their radial velocities, suggests that $V_i = 251 \pm 20 \text{ km s}^{-1}$ used in the present measurement of D is reasonable, or even a lower limit, without recourse to any modelling. For instance, if A1 and A2 are on the inside surface of the largest bipolar lobes, then their apparent positions in Fig. 1, without any other consideration, makes $\theta \gg 37^\circ$ (see Section 3) implausible.

The present PM observations show that *Hubble Space Telescope* images separated by $\geq 3 \text{ yr}$ will be needed to make further progress in the estimation of D by this PM technique. In any case, PM results from such imagery with an 0.1 arcsec resolution will have to be combined with (i) complete two-dimensional mapping of the radial velocity field (with an angular resolution of $\leq 1 \text{ arcsec}$) and (ii) detailed kinematical and morphological modelling to permit a more certain PM value of D to be derived.

ACKNOWLEDGMENTS

I wish to thank Dr Alberto López for his kind permission to reproduce his CCD images in Figs 2(a) and (b). Also I thank the plate library at the Royal Observatory Edinburgh for providing the 1954 POSS film copy and Dr Argyle at the Royal Greenwich Observatory for his precision scanning of the films with the PDS microdensitometer.

REFERENCES

- Hajian A. R., Terzian Y., 1996, *PASP*, 108, 419
 Hartigan P., Raymond J., Hartmann L., 1987, *ApJ*, 317, 323
 Huggins P. J., Bachiller R., Cox P., Forveille T., 1997, *ApJ*, 483, L57
 López J. A., Roth M., Tapia M., 1993a, *A&A*, 267, 194
 López J. A., Meaburn J., Palmer J. A., 1993b, *ApJ*, 415, L135
 López J. A., Vasquez R., Rodríguez L. F., 1995, *ApJ*, 445, L63
 López J. A., Meaburn J., Bryce M., Rodríguez L. F., 1997a, *ApJ*, 475, 705
 López J. A., Steffen W., Meaburn J., 1997b, *ApJ*, 485, L697
 Meaburn J., Walsh J. R., 1989, *A&A*, 223, 277
 Webster B. L., 1978, *MNRAS*, 185, 45p